Near-Continuous Profiling of Temperature, Moisture, and Atmospheric Stability Using the Atmospheric Emitted Radiance Interferometer (AERI)

W. F. FELTZ

Space Science and Engineering Center, Cooperative Institute for Meteorological Satellite Studies, University of Wisconsin—Madison, Madison, Wisconsin

W. L. SMITH

Atmospheric Sciences Division, NASA Langley Research Center, Hampton, Virginia

H. B. HOWELL, R. O. KNUTESON, H. WOOLF, AND H. E. REVERCOMB

Space Science and Engineering Center, Cooperative Institute for Meteorological Satellite Studies, University of Wisconsin—Madison, Madison, Wisconsin

(Manuscript received 7 January 2002, in final form 9 October 2002)

ABSTRACT

The Department of Energy Atmospheric Radiation Measurement Program (ARM) has funded the development and installation of five ground-based atmospheric emitted radiance interferometer (AERI) systems at the Southern Great Plains (SGP) site. The purpose of this paper is to provide an overview of the AERI instrument, improvement of the AERI temperature and moisture retrieval technique, new profiling utility, and validation of high-temporal-resolution AERI-derived stability indices important for convective nowcasting. AERI systems have been built at the University of Wisconsin—Madison, Madison, Wisconsin, and deployed in the Oklahoma–Kansas area collocated with National Oceanic and Atmospheric Administration 404-MHz wind profilers at Lamont, Vici, Purcell, and Morris, Oklahoma, and Hillsboro, Kansas. The AERI systems produce absolutely calibrated atmospheric infrared emitted radiances at one-wavenumber resolution from 3 to 20 μm at less than 10-min temporal resolution. The instruments are robust, are automated in the field, and are monitored via the Internet in near–real time. The infrared radiances measured by the AERI systems contain meteorological information about the vertical structure of temperature and water vapor in the planetary boundary layer (PBL; 0–3 km). A mature temperature and water vapor retrieval algorithm has been developed over a 10-yr period that provides vertical profiles at less than 10-min temporal resolution to 3 km in the PBL. A statistical retrieval is combined with the hourly Geostationary Operational Environmental Satellite (GOES) sounder water vapor or Rapid Update Cycle, version 2, numerical weather prediction (NWP) model profiles to provide a nominal hybrid first guess of temperature and moisture to the AERI physical retrieval algorithm. The hourly satellite or NWP data provide a best estimate of the atmospheric state in the upper PBL; the AERI radiances provide the mesoscale temperature and moisture profile correction in the PBL to the large-scale GOES and NWP model profiles at high temporal resolution. The retrieval product has been named AERIplus because the first guess used for the mathematical physical inversion uses an optimal combination of statistical climatological, satellite, and numerical model data to provide a best estimate of the atmospheric state. The AERI physical retrieval algorithm adjusts the boundary layer temperature and moisture structure provided by the hybrid first guess to fit the observed AERI downwelling radiance measurement. This provides a calculated AERI temperature and moisture profile using AERI-observed radiances ''plus'' the best-known atmospheric state above the boundary layer using NWP or satellite data. AERIplus retrieval accuracy for temperature has been determined to be better than 1 K, and water vapor retrieval accuracy is approximately 5% in absolute water vapor when compared with well-calibrated radiosondes from the surface to an altitude of 3 km. Because AERI can monitor the thermodynamics where the atmosphere usually changes most rapidly, atmospheric stability tendency information is readily available from the system. High-temporal-resolution retrieval of convective available potential energy, convective inhibition, and PBL equivalent potential temperature θ_e are provided in near–real time from all five AERI systems at the ARM SGP site, offering a unique look at the atmospheric state. This new source of meteorological data has shown excellent skill in detecting rapid synoptic and mesoscale meteorological changes within clear atmospheric conditions. This method has utility in nowcasting temperature inversion strength and destabilization caused by θ_e advection. This high-temporal-resolution monitoring of rapid atmospheric destabilization is especially important for nowcasting severe convection.

1. Introduction

The Space Science and Engineering Center (SSEC) at the University of Wisconsin—Madison, Madison, Wisconsin, has a 20-year history of developing aircraft and ground-based interferometer instrumentation and software to produce absolutely calibrated infrared radiances. These radiances are used to validate high-spectral-resolution line-by-line model calculations (Tobin et al. 1999; Clough et al. 1992) to retrieve profiles of atmospheric constituents (Smith et al. 1999; Feltz et al. 1998; He et al. 2001), and to derive cloud properties

Corresponding author address: W. F. Feltz, Space Science and Engineering Center, University of Wisconsin—Madison, 1225 West Dayton St., Rm. 239, Madison, WI 53715.
E-mail: wayne.feltz@ssec.wisc.edu

(Collard et al. 1995; Smith et al. 1998; DeSlover et al. 1999) and surface/oceanic skin properties (Smith et al. 1996; McKeown et al. 1995; Kearns et al. 2000; Minnett et al. 2001).

This paper focuses on an ongoing program at SSEC for using ground-based interferometric atmospheric radiance measurements to calculate the temperature and water vapor structure within the lower troposphere (the first 3 km of the atmosphere) and on the meteorological utility of this instrumentation. A ground-based two-channel interferometer system has been developed for the Department of Energy (DOE) Atmospheric Radiation Measurement Program (ARM; Stokes and Schwartz 1994). Known as the atmospheric emitted radiance interferometer (AERI; Revercomb et al. 1993), the instrument produces high-spectral-resolution radiances in the 3–20-μm region of the infrared spectrum at 1-wavenumber resolution. The AERI system is an absolutely calibrated (National Institute of Standards and Technology traceable) ground-based interferometer that yields absolute calibration accuracy to better than 1% of ambient radiance (Kearns et al. 2000; Minnett et al. 2001). The instrument is portable, robust, and field hardened and is monitored remotely via the Internet. The AERI instrument detects vertical and temporal changes of temperature and water vapor in the planetary boundary layer (PBL) through changes in the observed radiance spectrum. A less-than-10-min temporal resolution and 100-m vertical resolution in the lowest kilometer (degrading to 250-m resolution at 3 km) of the atmosphere (PBL) allows meteorologically important mesoscale features to be detected.

AERI participation in the ARM Program at the Southern Great Plains (SGP) site has allowed development of a robust operational atmospheric temperature and water vapor retrieval algorithm in a dynamic meteorological environment at five sites in Oklahoma and Kansas (Fig. 1). With AERI operating in a continuous mode, temperature and water vapor retrievals, obtained through inversion of the infrared radiative transfer equation, provide profiles of the atmospheric state every 10 min to 3 km in clear sky or below cloud base. The retrieval product has been named AERIplus because the first guess used for the mathematical physical inversion is derived from an optimal combination of statistical climatological, satellite, and numerical weather prediction model data, depending on the AERI system location. Boundary layer evolution, cold/warm frontal passages, drylines, and thunderstorm outflow boundaries have been observed, offering important meteorological information. By providing important vertical thermodynamic information between radiosonde locations and launch times, AERIplus retrievals provide data for stability index monitoring, planetary boundary layer research; and mesoscale model initialization, verification, and nowcasting. The AERI system represents an important new capability for operational weather and airport monitoring applications. The National Weather Service currently conducts special radiosonde launches to determine inversion strength and stability information prior to significant convective initiation. The AERIplus retrievals offer a way to monitor atmospheric stability at a less-than-10-min temporal resolution, providing important tendency information and forecast lead time. Coupled with a wind profiler or vertical azimuth display winds from a Doppler radar within a network, moisture convergence calculations show promise to predict the onset of precipitation (Petersen et al. 2000).

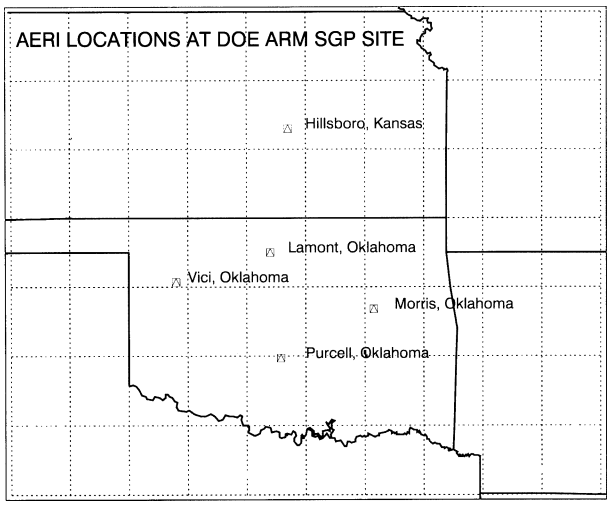

FIG. 1. A map of the AERI locations within the DOE ARM SGP site. DOE ARM AERI systems are also located near Barrow, Alaska (DOE ARM NSA site), and Nauru Island, South Pacific (DOE ARM TWP site).

2. AERI instrument description

The AERI instrument, shown in Fig. 2, is an advanced version of the high-resolution interferometer sounder designed and fabricated at the University of Wisconsin (Revercomb et al. 1988) to measure upwelling infrared radiances from an aircraft. AERI is a fully automated ground-based passive infrared interferometer that measures downwelling atmospheric radiance from 3.3 to 18.2 μm (550–3000 cm^{-1}) at a less-than-10-min temporal resolution with a spectral resolution of 1 wavenumber. Careful attention to calibration results in an absolute calibration accuracy of better than 1% of the ambient radiance. The AERI instrument foreoptics consist of a scene mirror and two calibration blackbodies. These blackbodies are essential to provide a well-known stable hot and ambient temperature reference for calibration of the downwelling sky-view radiances. A typical measurement cycle consists of a 3-min sky dwell period followed by 2-min dwell periods for each of the blackbodies. Although the interferometer acquires an uncalibrated spectrum every 2 s, averaging reduces the radiometric noise in the measurements. The temperature of one of the blackbodies is fixed at 60°C, while the other fluctuates with the ambient temperature.

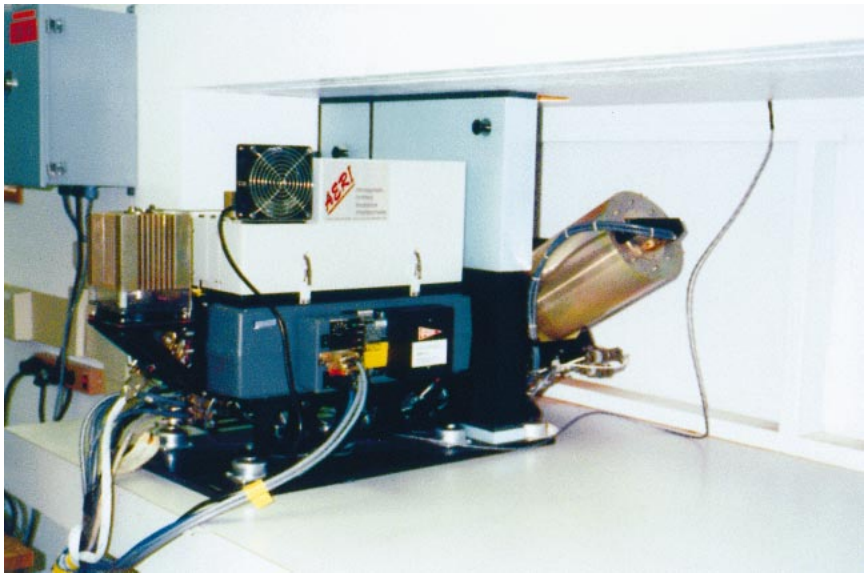

FIG. 2. The AERI instrument deployed at the DOE ARM SGP site.

Both of the AERI calibration reference sources are high-emissivity blackbody cavities that contain highly accurate temperature sensors. Calibration error analysis shows that for an instrument that must operate within an ambient atmospheric environment, the extrapolation of the hot–ambient calibration to the coldest ambient scene temperatures has a comparable accuracy to a calibration that makes use of a stable cold target (e.g., liquid nitrogen). This is because the temperature and emissivity uncertainty in reference cavities operated at or above ambient temperature can be made much smaller than those typically operated below the dewpoint temperature.

Because the AERI system performs a self calibration every 10 min, before and after each sky view, any temperature drifts in the ambient blackbody or the internal instrument temperature are accurately accounted for. One of the advantages of using an ambient calibration point is that much of the emission that the AERI measures is radiating from the atmosphere near the environmental ambient temperature. This means that the emission from near the surface is measured very precisely with the AERI instrument.

This hot–ambient approach greatly simplifies the operations of the instrument by removing the requirement for large amounts of liquid nitrogen to provide a cold calibration source (Revercomb et al. 1988). However, because the detector (a sandwiched HgCdTe/InSb detector, providing sensitivity for 5.5–18.2 and 3.3–5.5 μm in channels 1 and 2, respectively) requires cooling, a mechanical Stirling cooler has been employed. An example of an AERI-observed spectrum from channels 1 and 2 is shown in Fig. 3. The highlighted radiance regions indicate where the temperature (red) and water vapor (blue) profiles are derived using the physical retrieval algorithm discussed below.

3. Retrieval methodology and validation

The AERI downwelling radiance spectra contain vertical temperature and water vapor profile information above the AERI instrument, as documented in Feltz et al. (1998) and Smith et al. (1999). Through inversion of the radiative transfer equation, these profiles can be retrieved. However, the retrieval of water vapor and temperature from radiance data is an ill-posed problem. Smith (1970) provides an early example of how this problem was solved, and Feltz (1994) provides some background on the evolution of the retrieval technique. An iterative scheme is employed that makes use of a first-guess profile to perform a physical retrieval of the temperature and water vapor profiles (Smith et al. 1999). The lower–boundary layer first-guess profile is derived from a statistical methodology that is based on a regression of 1159 clear-sky radiosondes launched at the SGP central facility (near Lamont, Oklahoma) between 25 July 1994 and 10 May 1996 and a forward calculation at AERI spectral resolution using each of these radiosondes. The fast forward model (Garand et al. 2001) is a necessary component for performing AERIplus retrievals in real time (within a 10-min temporal window) and is obtained by regressing optical depth from a line-by-line transmittance model [in this case the Fast Atmospheric Signature Code (FASCODE) described in Clough et al. (1981)] against parameters obtained by temperature and water vapor mixing ratio profiles. The fast model essentially allows calculation of a radiance given an atmospheric temperature and moisture profile.

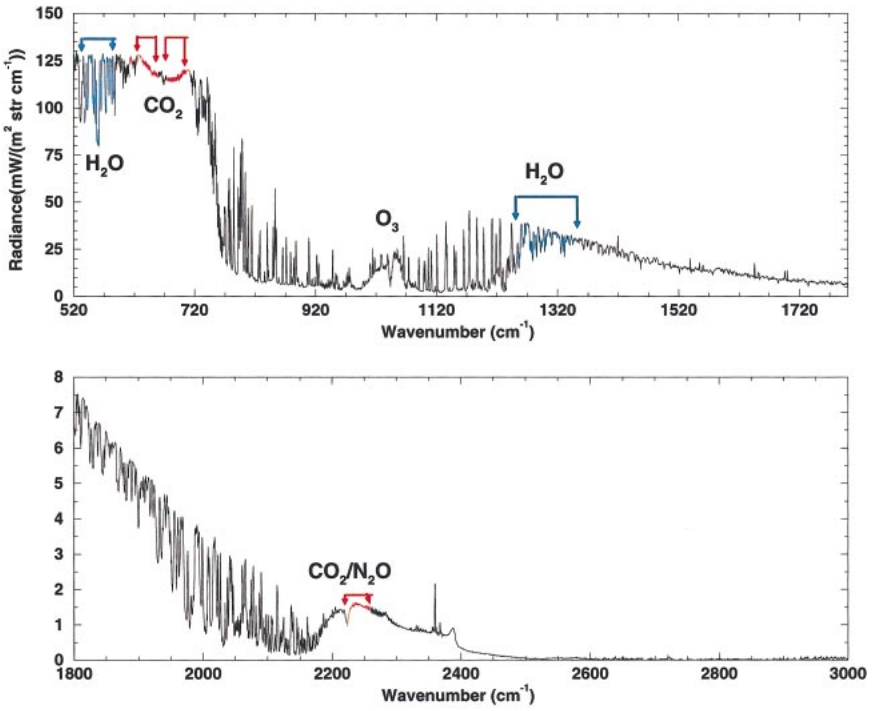

FIG. 3. An example of an AERI infrared radiance measurement at one-wavenumber resolution. The colored regions indicate the part of the spectrum in which temperature (red) and water vapor (blue) profiles are derived using the AERI physical retrieval algorithm.

In essence, the fast model allows an efficient way to translate atmospheric temperature and moisture profiles into radiance measurements. The first-guess regression of coefficients of temperature and moisture is very robust because it sampled many different meteorological events that passed through the SGP site domain. An observed AERI radiance spectrum is then passed through the regression coefficients (which relate the radiosonde temperature/moisture structure and forward calculations performed using the radiosonde profiles), providing a first guess of atmospheric state in the lower PBL. This first guess of temperature and moisture based upon site-specific climatological data is then passed through a physical retrieval algorithm described by Smith et al. (1999). The spectral regions used to perform the physical retrieval are shown in Fig. 3. Because of the strength of the IR signal at the surface from emission within the lower atmosphere, the weighting functions become broad at 2.5–3.0 km, and thus the retrievals using only AERI data are limited to below this altitude.

The statistical first guess derived from a regression database that relates radiosonde profiles and fast model radiance calculations provides an adequate definition of temperature and moisture in the lower PBL. However, the first guess rapidly converges to the mean temperature and moisture profile of the statistical radiosonde regression (the mean temperature and moisture profile of the 1159 radiosondes) in the upper PBL (above 2 km) because the observed AERI radiance lacks temperature and moisture profile information above the PBL. An optimal full-tropospheric first guess of the atmospheric state can be derived by combining the following sources of atmospheric information:

1) a statistical methodology that is based on a regression of cloud-free radiosondes and a forward calculation at AERI spectral resolution using each of these radiosondes,
2) satellite-based retrievals of temperature and moisture,
3) the best numerical weather prediction (NWP) model hourly analysis of temperature and moisture, and
4) temporally interpolated radiosonde temperature and moisture profiles (if available).

The approach involves producing the optimal first guess using a priori, remotely sensed, or NWP model thermodynamic atmospheric state information. The optimal first guess is site dependent because time-interpolated radiosonde data (if available) may be the only alternative in remote regions where satellite or NWP data are not available. Over the SGP domain, satellite and NWP models both provide excellent mid-/upper-tropospheric atmospheric-state information for the AERI first guess.

The first attempt to optimize the AERI-retrieval first guess implemented Geostationary Operational Environmental Satellite (GOES)-sounder temperature and moisture profiles to supplement the statistical first guess from

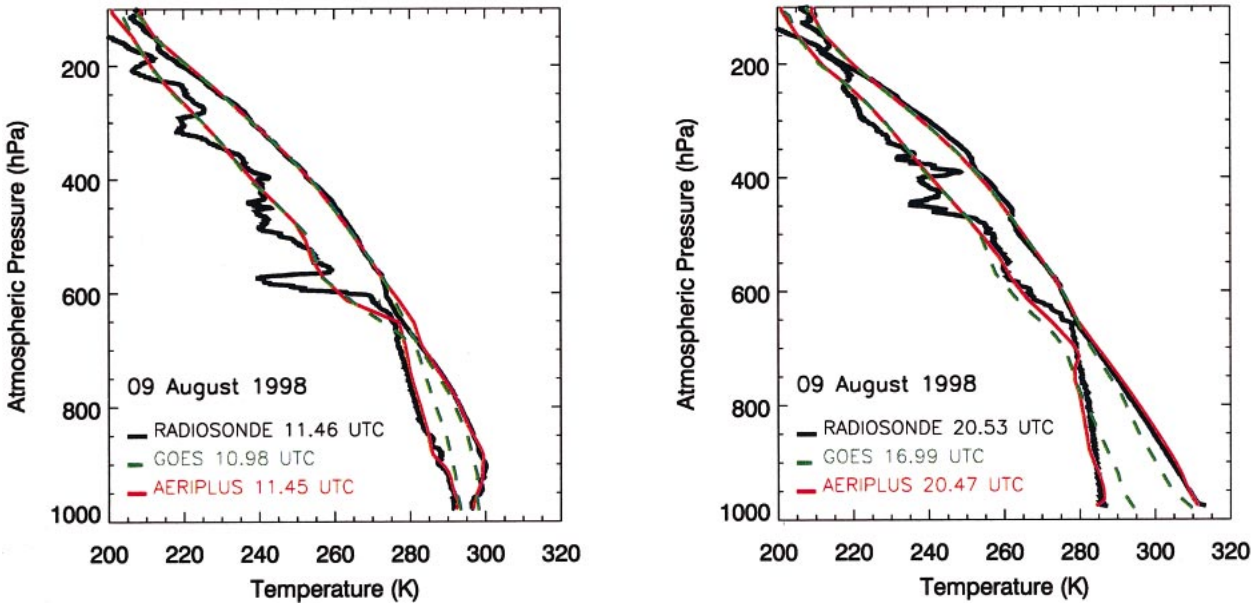

FIG. 4. A comparison of radiosondes (black lines) with the nearest GOES retrievals (dashed green lines) in time and space and the final AERIplus physical retrievals (red lines) at (left) 1130 and (right) 2030 UTC on 9 Aug 1998. The right lines for each colored pair are temperature profiles, and the left lines are dewpoint temperature (moisture) profiles.

2 km to the top of the troposphere. GOES-sounder 30 km × 30 km retrievals of water vapor and temperature are produced hourly by the Cooperative Institute for Meteorological Satellite Studies at the University of Wisconsin—Madison over all five of the SGP site facilities. These GOES retrievals of temperature and water vapor have been used to serve as the first guess of the atmospheric state from the upper PBL (2.5 km) to the tropopause (Turner et al. 2000; Schmit et al. 2002). The first guess (derived from the GOES-sounder upper- and midtropospheric profile and AERI statistical retrieval in the PBL, where the two are linearly blended between 2 and 3 km) is passed through the physical retrieval, iterating to a solution that satisfies the observed infrared radiance. Figure 4 shows an example of the nearest GOES-sounder retrieval (dashed green lines) and final AERI + GOES physical retrieval (red lines) in comparison with radiosondes (black lines) launched on 9 August 1998. Note how the AERIplus physical retrieval algorithm adjusted the temperature and dewpoint temperature to within good agreement to the radiosonde. In essence, the observed AERI radiances defined the mesoscale boundary layer thermodynamic state at the AERI location.

These GOES retrievals use the Eta NWP forecast model (Black 1994) as a first guess of atmospheric state. The initial analysis from the Eta Model is updated every 12 h; thus, the first guess used for the GOES physical retrieval is based on a forecast until the time of the next analysis cycle (Schmit et al. 2002). The GOES-sounder profiles provide a viable first guess of atmospheric state; however, GOES retrievals are not available during periods of high, thick cirrus and altostratus clouds. This causes a lack of hourly GOES-sounder profiles during thick upper-level cloud cover, which is a disadvantage to the AERI ground-based profiling technique because temperature and moisture retrievals are possible to cloud base with a sufficient estimate of atmospheric state and a cloud-base altitude. A more routine update of the atmospheric state in the mid- and upper troposphere can be provided by an NWP model analysis, as long as sufficient prior data are used by the model.

In the operational setting, the AERIplus retrievals derived at the ARM SGP site now incorporate hourly Rapid Update Cycle, version 2, (RUC-2; Benjamin et al. 1994, 1995) NWP analysis profiles into the first guess, instead of GOES-sounder profiles. The RUC-2 NWP model's initial analysis is updated hourly using remotely sensed and in situ data (GOES-sounder total precipitable water and cloud-top pressure, aircraft temperature reports, wind-profiler data, etc.). These operational RUC-2 NWP model data streams, made available on the Internet from the Forecast Systems Laboratory (FSL), provide a better first guess of temperature than the Eta temperature forecasts (the temperature profiles within the GOES-sounder data stream) as a result of the hourly data assimilation. GOES-sounder three-layer integrated water vapor is also ingested into the hourly FSL RUC-2 data assimilation, providing the best a priori first guess over the ARM SGP site domain. The statistical first guess derived from the observed AERI radiance is blended into hourly RUC-2 NWP initial-analysis water vapor and temperature fields to provide a hybrid best estimate of atmospheric state to the AERI physical retrieval (the new retrieval product is named AERIplus because it incorporates the best-known atmospheric

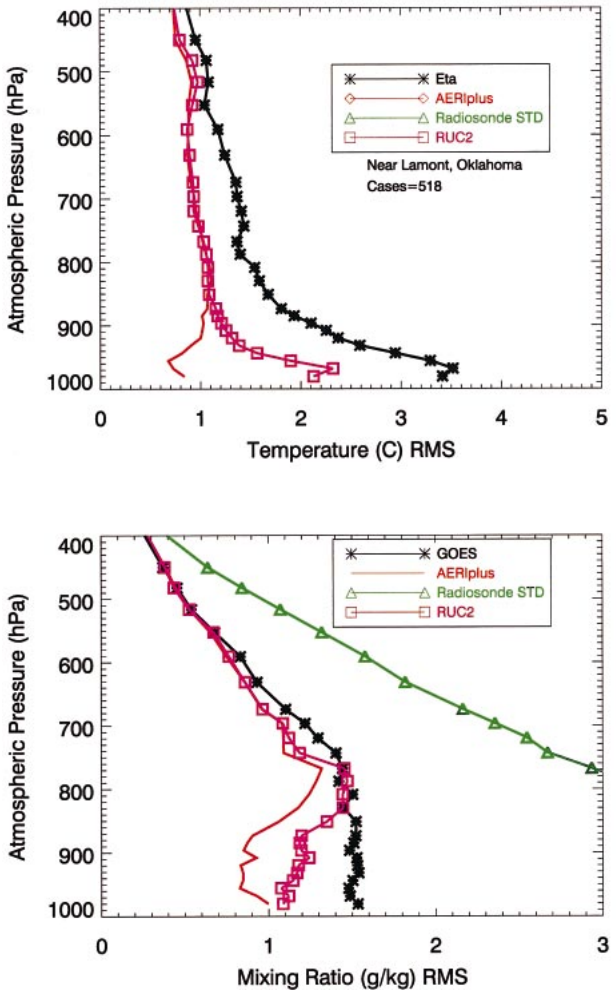

FIG. 5. A comparison of (top) temperature and (bottom) mixing ratio rms differences from 518 Vaisala radiosonde launches and Eta/GOES (star/black), RUC-2 (square/magenta), and physically retrieved AERIplus profiles (no symbol/red) for Mar–Dec 2000 at the central SGP site facility. A green line indicates the radiosonde std dev (triangle/green) for temperature and mixing ratio during this period, if within *x* axis domain (temperature std dev is greater than 5°C for temperature comparison).

state from radiosonde regression, satellite, and NWP data sources to provide the optimal first guess to the physical retrieval algorithm). The 40-km resolution of the RUC-2, however, does not accurately portray the PBL thermodynamic state at a particular location. For example, nocturnal temperature inversion intensity is often in error, and boundary layer moisture biases are sometimes present in NWP analyses and forecasts. The AERIplus physical retrieval algorithm acts to change the estimated temperature and moisture structure given by this hybrid first guess to fit the observed infrared radiance measurements through a form of the infrared radiative transfer equation (Smith et al. 1999; Feltz et al. 1998).

Figure 5 (top panel) shows the improvement that the AERIplus physical retrieval (red) offers to the first-guess temperature over the RUC-2 hourly initial analysis (magenta) and Eta hourly forecast/analysis data (black) for 522 radiosonde matches from March to December 2000. Note that the AERIplus retrievals show rms differences that are 1 K or less when compared with radiosondes. In contrast, the RUC-2 and Eta NWP models show increasing error within the boundary layer. Figure 5 (bottom panel) shows the water vapor mixing ratio rms differences between AERIplus, RUC-2, and GOES-sounder water vapor profiles as compared with radiosondes. Modest improvement over RUC-2 and GOES is indicated within the PBL by the AERIplus physical retrieval. Note that AERIplus retrievals are available at less-than-10-min intervals between the hourly upper-level first-guess information (statistical retrievals are updated every 10 min also, because they are based on the observed AERI radiances).

Extensive validation of the AERIplus water vapor profiles as compared with microwave-scaled radiosondes [to account for known Vaisala, Inc., radiosonde dry bias explained within Revercomb et al. (2003)] indicates an absolute rms mixing ratio difference of 5% (Turner et al. 2000). Consider the inherent differences between the measurement systems:

1) radiosonde-to-radiosonde variability in calibration (Revercomb et al. 2003; Turner et al. 2003);
2) radiosonde dry bias in water vapor measurements (Guichard et al. 2000; Wang et al. 2002; Turner et al. 2003; Revercomb et al. 2003);
3) variance in surface and PBL temperature/moisture horizontally, even in close proximity (Weckwerth 2000); and
4) differences in space and time between a moving-point measurement (radiosonde) and a column measurement (AERIplus).

The water vapor retrieval differences indicate high skill after considering the different measurement methodologies between the systems and the high temporal variation of water vapor both horizontally and vertically within the PBL.

The high-temporal-resolution AERIplus temperature and moisture profiles provide powerful nowcasting diagnostic and NWP model validation data. Examples of time–height cross sections of several mesoscale meteorological events are shown in Fig. 6. A cold-frontal passage (top panel, between 1000 and 1400 UTC), elevated mixed layer (middle panel, between 0800 and 2400 UTC), and dryline event (lower panel, between 0900 and 1200 UTC) are all captured by the AERIplus retrievals. The 915-MHz wind-profiler data have been plotted on the cold-frontal and dryline passage examples to show the high correlation between the independently remotely sensed wind and the AERIplus thermodynamic field.

A demonstration of RUC-2 initial-analysis validation is provided in Fig. 7. These time–height cross sections

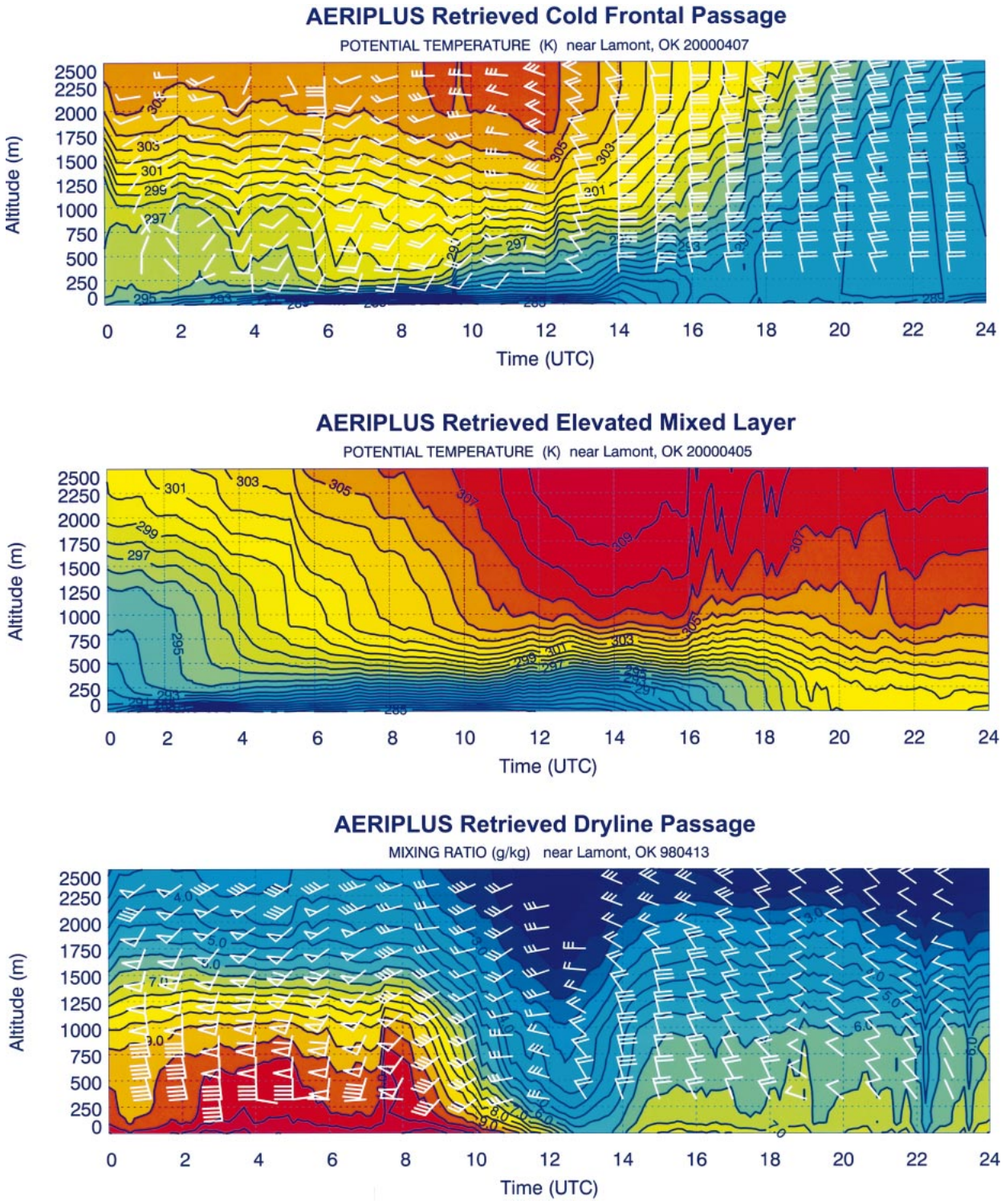

FIG. 6. AERIplus-retrieved thermodynamic meteorological events for a (top) cold front, (middle) elevated mixed layer, and (bottom) dryline passage. The winds plotted over the AERIplus time–height cross section were obtained from a collocated 404-MHz wind profiler.

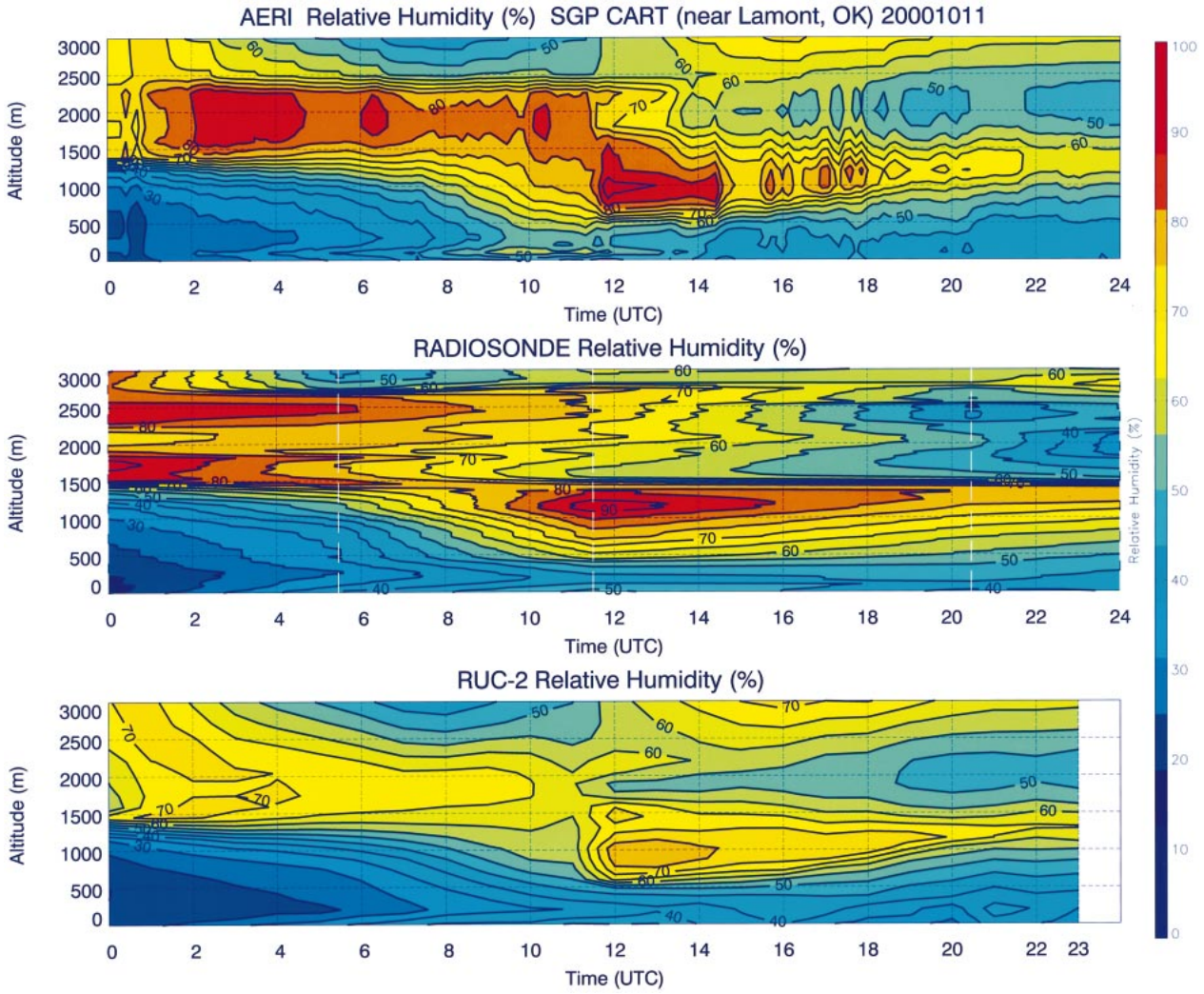

FIG. 7. Time–height cross sections of relative humidity from (top) the AERI instrument, (middle) radiosondes, and (bottom) the RUC-2 NWP model on 11 Oct 2000. The time resolution for the AERIplus profiles is less than 10 min, white lines indicate radiosonde launches, and the RUC-2 data are the hourly analysis.

provide a sample of 10-min AERIplus, radiosonde, and hourly RUC-2 time series of relative humidity from 11 October 2000. The five radiosonde launch times are indicated by the white dashed lines, and a linear interpolation of the relative humidity is displayed between the launch times. Notice that although the humidity structure within all three cross sections is similar, the magnitudes of the relative humidity values are too low in the RUC-2 analysis of hourly relative humidity cross section relative to the AERIplus or radiosonde cross section.

Several algorithms have been developed to postprocess the AERIplus retrievals, including those to derive 10-min atmospheric stability (next section) and a mixed boundary layer mask (Fig. 8) (the colored area essentially maps out the area on a time series for which the vertical running standard deviation of the potential temperature is less than 0.5 K). These products indicate the potential for development of NWP/climate model parameterizations using this high-time-resolution boundary layer thermodynamic information.

4. Atmospheric stability monitoring and case studies

The determination of water vapor mixing ratio and temperature profiles within the boundary layer with AERIplus retrievals enables high temporal monitoring of stability indices. The AERIplus retrievals can determine average (the lowest 100 hPa of atmosphere) parcel equivalent potential temperature θ_e very accurately because the transmission of infrared radiation from moisture and carbon dioxide is occurring close to the instrument scene mirror. Because the water vapor mixing ratio/temperature profile and average (first 100 hPa of atmosphere) bulk equivalent potential energy can be

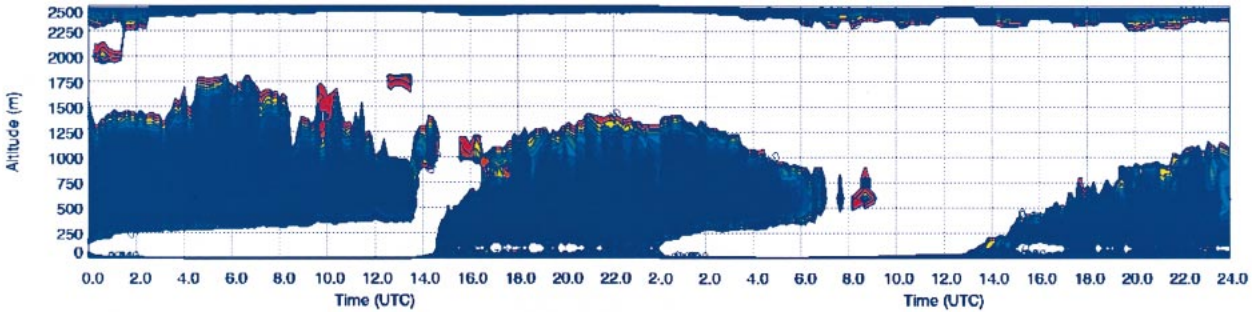

FIG. 8. A time series of vertical variation of potential temperature during a 2-day period from the recent water vapor intensive observation period in 2000 (Revercomb et al. 2003). The colored regions indicate where the potential temperature varies by less than 0.5 K, effectively mapping out the bottom of the PBL entrainment zone and residual layers defined by the AERIplus temperature retrievals.

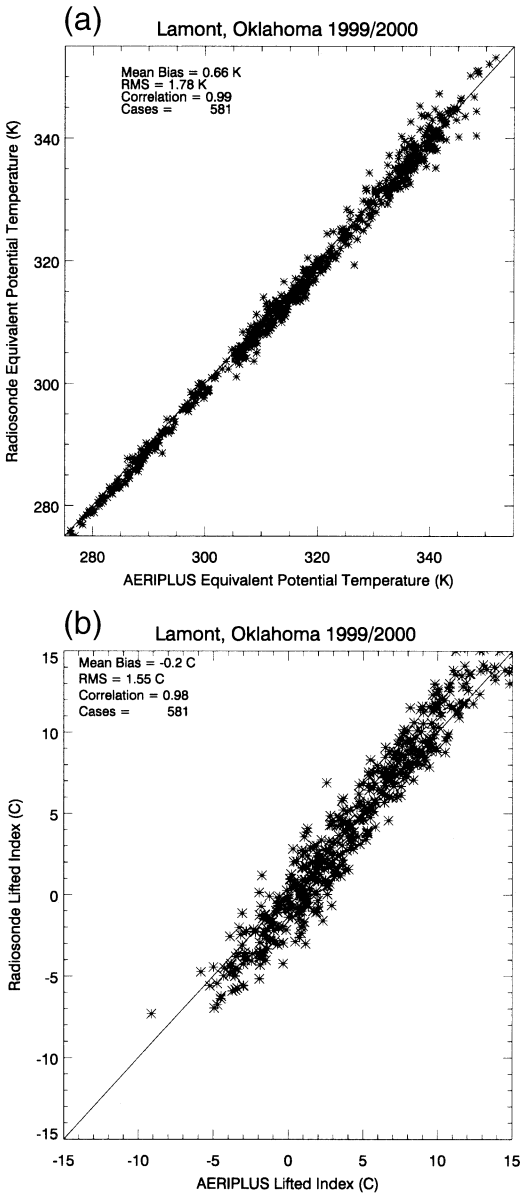

FIG. 9. A scatterplot of AERIplus-derived avg lowest 100-hPa parcel (a) θ_e and (b) lifted index vs coincident radiosondes for 581 cases.

monitored continuously (except during precipitation and fog), most other common stability indices can be derived with a representative temperature profile of the current atmospheric state. The boundary layer temperature structure can be resolved using the AERIplus retrievals, including monitoring of elevated temperature inversions. The balance between the magnitude of the convective available potential energy (CAPE) and the convective inhibition (CIN; regulated primarily by the intensity of a ''capping'' temperature inversion) is currently monitored only with National Weather Service radiosonde launches. The AERIplus retrievals allow a means to observe rapid destabilization and moisture magnitude, which contribute directly to realizing any existing convective available potential energy.

The AERIplus-derived atmospheric stability information has been validated using 581 coincident radiosondes near Lamont, Oklahoma, during the spring/summer of 1999 and 2000. Figure 9a shows a scatterplot of the average lowest 100-hPa parcel θ_e for radiosondes on the *y* axis and AERIplus retrievals on the *x* axis. An excellent correlation of 0.99 and an rms difference of less than 2 K are noted. Figure 9b shows similar agreement for the lifted index. Correlation was determined to be 0.98 with an rms difference of approximately 1.5°C. To determine an accurate lifted index or CAPE value, the temperature profile above the boundary layer is used (provided by the RUC-2 analysis).

Two case studies demonstrate how the AERIplus retrievals quantitatively monitored rapid atmospheric destabilization. In the first case, CIN was rapidly reduced because of moisture advection on 24 May 1998. A supercell thunderstorm with an F3 (on the Fujita–Pearson scale) tornado developed and passed in close proximity to the DOE ARM SGP central facility near the location of the AERI system. In the second case, a rapid cooling of the elevated temperature inversion was observed with the AERIplus retrievals during the 3 May 1999 Oklahoma–Kansas tornado outbreak.

a. 24 May 1998

The higher temporal resolution provided by the AERIplus retrieval product reveals an important new

source of meteorological data to the forecaster. Figure 10 shows AERIplus water vapor retrievals in the PBL, along with a less-than-10-min-temporal-resolution parcel θ_e, lifted index, CAPE, and CIN on 24 May 1998. A cold front had moved through northern Oklahoma, drying and stabilizing the atmosphere between 0000 and 1200 UTC. The front moved back to the north as a warm front, indicated by the superimposed National Oceanic and Atmospheric Administration (NOAA) 404-MHz wind-profiler wind barbs (winds veer from easterly to southeasterly between 1200 and 1600 UTC), and brought a rapid advection of moisture within the PBL between 1600 and 2400 UTC.

Rapid destabilization of the atmosphere at a less-than-10-min resolution is shown where the lifted index decreases from 0°C at 1200 UTC to −10°C at 2400 UTC. A rapid rise in CAPE values from 0 J kg^{-1} at 1600 UTC to 5000 J kg^{-1} at 2400 UTC indicates the rapid increase in energy available for explosive convection. Most important is that the AERIplus retrievals provide an excellent method for monitoring the inversion inhibiting the thunderstorm development. This is indicated by the CIN values of near −900 J kg^{-1} at 1600 UTC (not shown), which rapidly diminish at 2400 UTC. The rapid decay of the CIN was caused not by erosion of the inversion but rather by a rapid moisture increase due to advection. An important note is that no radiosondes were launched from the SGP site on 24 May 1998 because it was a Sunday. These data were derived entirely through remote sensing of the infrared spectrum. A supercell developed northwest of the SGP site at 2330 UTC, spawning an F3-intensity tornado that occurred within 5 km of the site location. Additional information can be found in Lehmiller et al. (2000).

b. 3 May 1999

On 3 May 1999 at least 63 tornadoes were reported in the states of Oklahoma and Kansas. One F5 tornado tracked through the southern suburbs of Oklahoma City, Oklahoma, destroying approximately 10 000 homes and businesses. More than 50 people lost their lives in Oklahoma and Kansas because of this outbreak (Speheger et al. 2002).

Two of the AERI instruments, one in Lamont, Oklahoma, and the other in Purcell, Oklahoma, retrieved the decrease in CIN just prior to the onset of the severe convection. Figure 11 indicates this trend in CIN first at Purcell between 1900 and 2100 UTC and next at Lamont in north-central Oklahoma between 2300 and 2400 UTC. The lowering of CIN at Purcell, between about 1900 and 2100 UTC, corresponds to the rapid development of thunderstorms in regions south and west of Oklahoma City during this time period. The location and time of initiation of the first supercell thunderstorms were southwest of Lawton, Oklahoma, at approximately 2030 UTC. At Lamont, CIN decreased gradually from −180 to −50 J kg^{-1} from 1900 to about 2300 UTC 3 May, before rapidly decreasing to −25 J kg^{-1} by 2330 UTC. Note that, although high temporal monitoring of CIN is useful for operational forecaster nowcasting, CIN is only one part of the thunderstorm initiation problem. Parcel lift may be high enough to overcome CIN (Thompson and Edwards 2000).

There are two primary ways CIN can rapidly decrease. The first possibility is rapid destabilization caused by PBL heating and moisture advection, the other is the rapid erosion of the temperature inversion. Notice on Fig. 11a that the average lowest 100-hPa parcel θ_e at both of these sites slowly increases. Figure 12 indicates that the rapid erosion of the temperature inversion is present in the AERIplus retrievals as well as two radiosondes launched by the DOE ARM Program on the afternoon of 3 May 1999, leading to the resultant decrease in CIN. In this case, the real-time AERI stability information would not have enhanced forecasters' knowledge of exact thunderstorm development because the systems were not located near the Lawton area. However, stability tendency and AERI location stability comparisons may help the forecaster to define better the region of expected convective development. Additional information about this study can be found in Feltz and Mecikalski (2002).

The two case studies discussed above indicate the ability of the AERI system and algorithm to monitor the equivalent potential energy in the PBL and the capping temperature inversion. The ability to monitor the balance between these two features at high temporal resolution is a key to nowcasting convective initiation. High-temporal-frequency monitoring of the capping temperature inversion and average boundary layer equivalent potential temperature is currently not available operationally to National Weather Service meteorologists. Instead, special non-synoptic-time radiosonde launches are requested, and/or morning radiosonde data are modified with NWP forecast knowledge or predicted high temperature to estimate capping inversion strength and boundary layer equivalent potential energy. Real-time AERI-derived stability indices and atmospheric state profiles could be found online (http://cimss.ssec.wisc.edu/aeriwww/aeri/aeri.html) at the time of writing.

5. Conclusions

The AERI instrument has been made operational at the DOE ARM sites over a 10-year period. A mature temperature and moisture retrieval algorithm has evolved to allow near-continuous profiling of those parameters within the PBL in a clear sky or to the cloud base. Several satellite and NWP thermodynamic products have been used to improve the first guess of the atmospheric state from the upper PBL to the tropopause. These a priori data provide the AERIplus physical retrieval with a better estimate of the atmospheric state, which allows better convergence to the true boundary layer temperature and moisture structure. The AERI ra-

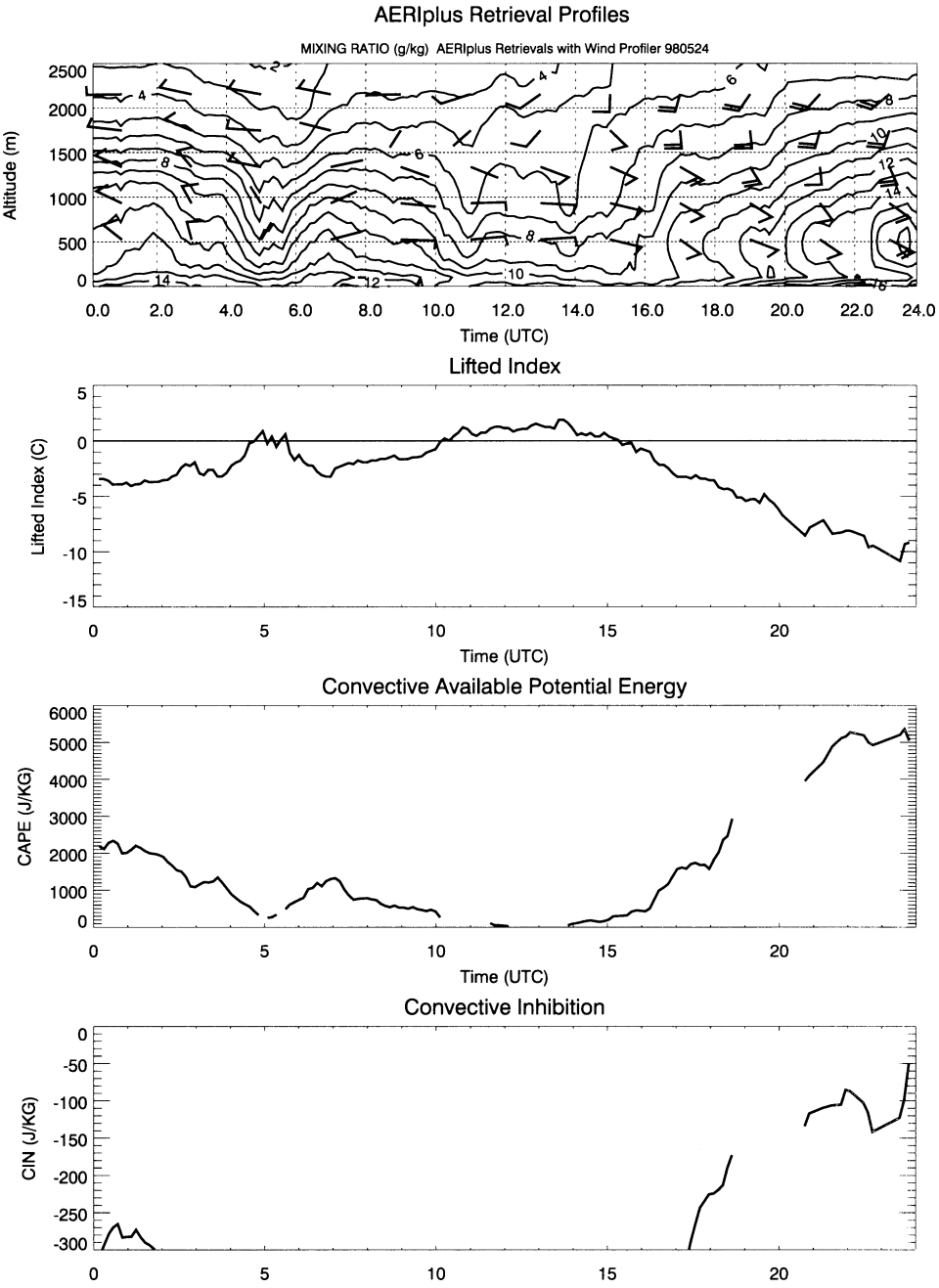

FIG. 10. (top) A time–height cross section of AERIplus-derived water vapor mixing ratio retrieved on 24 May 1998. Wind-profiler winds are plotted over this cross section. Between 0000 and 1200 UTC substantial drying is indicated in the PBL from a cold-frontal passage. Rapid moistening is indicated as the front retreats back to the north as a warm front. The lower three panels show the stability indices calculated for this time period from AERIplus retrievals. Rapid destabilization is noted between 1500 and 2400 UTC prior to a tornado occurrence.

diances provide the boundary layer mesoscale information at high temporal resolution that 30-km GOES-sounder or 40-km RUC-2 profiles are lacking. Temperature retrieval rms differences are 1 K or less and absolute water vapor mixing ratio differences are approximately 5% when compared with ARM radiosonde launches near Lamont. The AERI systems provide a powerful new data source to quantify mesoscale information for the forecaster. Examples indicating good skill in AERIplus retrieval calculation of bulk equivalent potential temperature, convective inhibition, lifted index, and mapping boundary layer mixed layers were

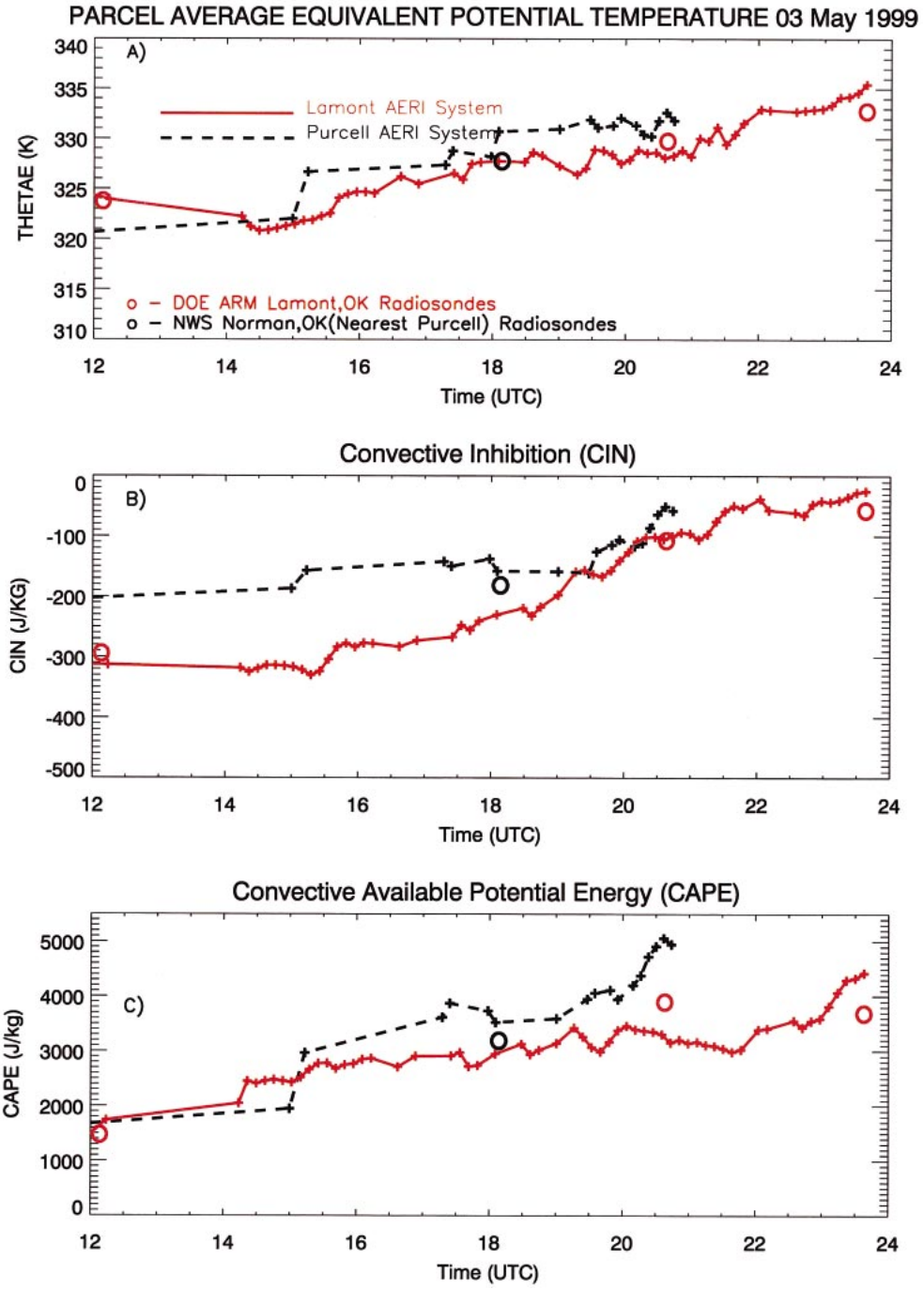

FIG. 11. Time series of (top) θ_e, (middle) CIN, and (bottom) CAPE derived from AERIplus retrievals for Purcell, Lamont, and Vici, OK, on 3 May 1999. Circles indicate validation radiosonde data points. Notice the rapid decrease of CIN, first at Purcell and then at Lamont, caused by the rapid erosion of the temperature inversion between 2000 and 2100 and 2300 and 2400 UTC, respectively.

presented and provide a unique validation and forecasting resource, which is now being demonstrated in the DOE ARM SGP region.

It is understood that real-time monitoring of atmospheric stability provides only part of the answer relating to convective initiation. High-temporal/spatial-resolution wind profiles are needed to monitor convergence/advection of the moist static energy. Future work includes validation of horizontal moisture flux advection and divergence calculations provided by AERI and collocated wind-profiler measurements (Petersen et al. 2000) within the SGP site domain. The combination of

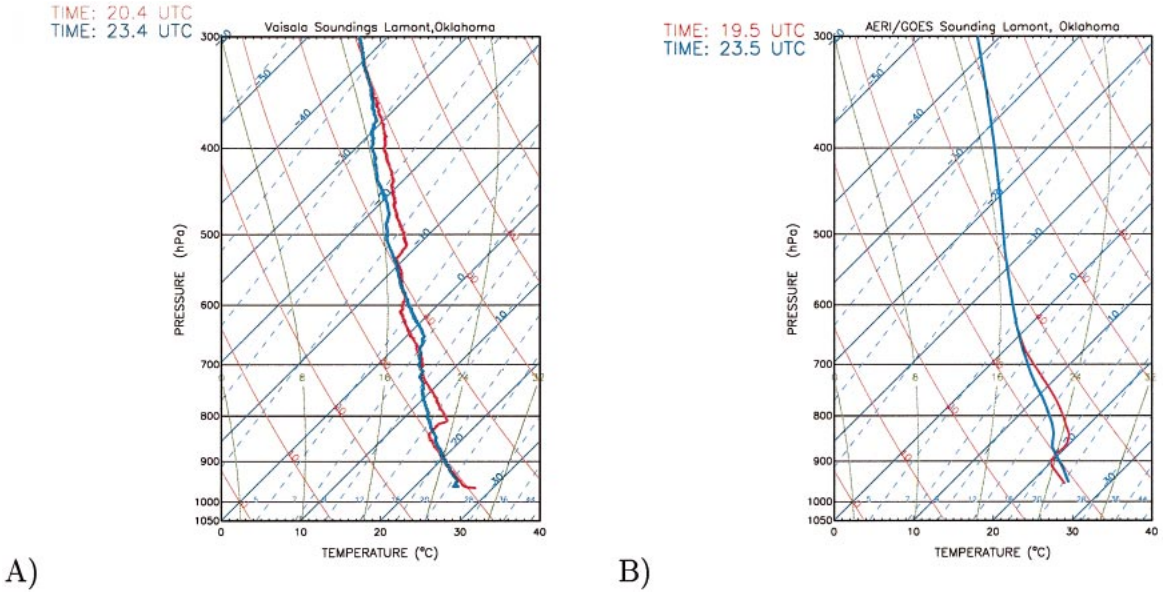

FIG. 12. A comparison of temperature profiles from (a) two radiosondes and (b) AERIplus retrievals near Lamont. The radiosondes were launched at 2030 and 2330 UTC, respectively, and the retrievals were from 2000 and 2330 UTC. Both indicate the loss of the capping temperature inversion. The AERIplus Purcell retrievals were consistent with the Lamont profiles.

the AERIplus moisture and temperature information with wind-profiler observations facilitates detailed studies of the dynamical processes involved in modifying the preconvective environment and focusing the energy needed to subsequent convection. An automated technique to calculate moisture flux between the site locations will be developed for forecast evaluation. In addition, there is work in progress to deploy a network of AERI systems along the Gulf of Mexico to detect the depth and magnitude of moisture return flow into the central United States. Such a network would provide operational meteorologists and NWP models better and more frequent quantitative moisture information than is currently available from the sparse radiosonde network near the Gulf of Mexico.

Acknowledgments. This work was funded by the Atmospheric Radiation Measurement Program (DE-FG02-92ER61365) and the National Oceanic and Atmospheric Administration (NOAA Grant NA67EC0100). Data were obtained by the ARM Program sponsored by the U.S. Department of Energy Office of Science, Office of Biological and Environmental Research, Environmental Sciences Division.

REFERENCES

Benjamin, S. G., K. J. Brundage, and L. L. Morone, 1994: The Rapid Update Cycle. Part I: Analysis/model description. NOAA/NWS Tech. Procedures Bull. 416, 16 pp. [Available from National Weather Service, Office of Meteorology, 1325 East-West Highway, Silver Spring, MD 20910.]

——, D. Kim, and T. W. Schlater, 1995: The Rapid Update Cycle: A new mesoscale assimilation system in hybrid theta–sigma coordinates at the National Meteorological Center. Preprints, *Second Int. Symp. on Assimilation of Observations in Meteorology and Oceanography*, Tokyo, Japan, Japanese Meteorological Agency, 337–342.

Black, T. L., 1994: The new NMC Mesoscale Eta Model: Description and forecast examples. *Wea. Forecasting,* **9,** 265–284.

Clough, S. A., F. X. Kneizys, L. S. Rothman, and W. O. Gallery, 1981: Atmospheric spectra transmittance and radiance: FASCODE1B. *SPIE Atmos. Trans.*, **277,** 152–166.

——, M. J. Jacono, and J. L. Moncet, 1992: Line-by-line calculations of atmospheric fluxes and cooling rates: Application to water vapor. *J. Geophys. Res.,* **97,** 15 761–15 785.

Collard, A. D., S. A. Ackerman, W. L. Smith, X. Ma, H. E. Revercomb, R. O. Knuteson, and S.-C. Lee, 1995: Cirrus cloud properties derived from high spectral resolution infrared spectrometry during FIRE II. Part III: Ground-based HIS results. *J. Atmos. Sci.,* **52,** 4264–4275.

DeSlover, D. H., W. L. Smith, P. K. Piironen, and E. W. Eloranta, 1999: A methodology for measuring cirrus cloud visible-to-infrared spectral optical depth ratio. *J. Atmos. Oceanic Technol.,* **16,** 251–262.

Feltz, W. F., 1994: Meteorological applications of the atmospheric emitted radiance interferometer (AERI). M.S. thesis, Dept. of Atmospheric and Oceanic Sciences, University of Wisconsin—Madison, 87 pp. [Available from University of Wisconsin—Madison, Schwerdtfeger Library, 1225 W. Dayton, Madison, WI 53706.]

——, and J. R. Mecikalski, 2002: Monitoring high-temporal-resolution convective stability indices using the ground-based atmospheric emitted radiance interferometer (AERI) during the 3 May 1999 Oklahoma–Kansas tornado outbreak. *Wea. Forecasting,* **17,** 445–455.

——, W. L. Smith, R. O. Knuteson, H. E. Revercomb, H. M. Woolf, and H. B. Howell, 1998: Meteorological applications of temperature and water vapor retrievals from the ground-based atmospheric emitted radiance interferometer (AERI). *J. Appl. Meteor.,* **37,** 857–875.

Garand, L., and Coauthors, 2001: Radiance and Jacobian intercomparison of radiative transfer models applied to HIRS and AMSU channels. *J. Geophys. Res.,* **106,** 24 017–24 031.

Guichard, F., D. Parsons, and E. Miller, 2000: Thermodynamic and radiative impact of the correction of humidity sounding bias in the Tropics. *J. Climate,* **13,** 3611–3624.

He, H., W. W. McMillan, R. O. Knuteson, and W. F. Feltz, 2001: Tropospheric carbon monoxide column density retrieval during the pre-launch MOPITT validation exercise. *Atmos. Environ.,* **35,** 509–514.

Kearns, E. J., J. A. Hanafin, R. H. Evans, P. J. Minnett, and O. B. Brown, 2000: An independent assessment of Pathfinder AVHRR sea surface temperature accuracy using the marine atmosphere emitted radiance interferometer (MAERI). *Bull. Amer. Meteor. Soc.,* **81,** 1525–1536.

Lehmiller, G. S., H. B. Bluestein, P. J. Neiman, F. M. Ralph, and W. F. Feltz, 2001: Wind structure in a supercell thunderstorm as measured by a UHF wind profiler. *Mon. Wea. Rev.,* **129,** 1968–1986.

McKeown, W., F. Bretherton, H. L. Huang, W. L. Smith, and H. L. Revercomb, 1995: Sounding the skin of water: Sensing air–water interface temperature gradients with interferometry. *J. Atmos. Oceanic Technol.,* **12,** 1313–1327.

Minnett, P. J., R. O. Knuteson, F. A. Best, B. J. Osborne, J. A. Hanafin, and O. B. Brown, 2001: The marine-atmospheric emitted radiance interferometer: A high-accuracy, seagoing infrared spectroradiometer. *J. Atmos. Oceanic Technol.,* **18,** 994–1013.

Petersen, R. A., W. F. Feltz, J. Schaefer, and R. Schneider, 2000: An analysis of low-level moisture-flux convergence prior to the 3 May 1999 Oklahoma City tornadoes. Preprints, *Proc. 20th Conf. on Severe Local Storms,* Orlando, FL, Amer. Meteor. Soc., 619–621.

Revercomb, H. E., H. Buijs, H. B. Howell, D. D. LaPorte, W. L. Smith, and L. A. Sromovsky, 1988: Radiometric calibration of IR Fourier transform spectrometers: Solution to a problem with the High Resolution Interferometer Sounder. *Appl. Opt.,* **27,** 3210–3218.

——, F. A. Best, R. G. Dedecker, T. P. Dirkx, R. A. Herbsleb, R. O. Knuteson, J. F. Short, and W. L. Smith, 1993: Atmospheric emitted radiance interferometer (AERI) for ARM. Preprints, *Fourth Symp. on Global Climate Change Studies,* Anaheim, CA, Amer. Meteor. Soc., 46–49.

——, and Coauthors, 2003: The Atmospheric Radiation Measurement (ARM) Program's water vapor intensive operational periods: Overview, accomplishments, and future challenges. *Bull. Amer. Meteor. Soc.,* **84,** 217–236.

Schmit, T. J., W. F. Feltz, W. P. Menzel, J. Jung, A. P. Noel, J. N. Heil, J. P. Nelson III, and G. S. Wade, 2002: Validation and use of GOES sounder moisture information. *Wea. Forecasting,* **17,** 139–154.

Smith, W. L., 1970: Iterative solution of the radiative transfer equation for the temperature and absorbing gas profile of an atmosphere. *Appl. Opt.,* **9,** 1993–1999.

——, and Coauthors, 1996: Observations of the infrared radiative properties of the ocean—Implications for the measurements of sea surface temperature via satellite remote sensing. *Bull. Amer. Meteor.,* **77,** 41–51.

——, S. A. Ackerman, H. E. Revercomb, H. L. Huang, D. H. DeSlover, W. F. Feltz, L. Gumley, and A. Collard, 1998: Infrared spectral absorption of nearly invisible cirrus clouds. *Geophys. Res. Lett.,* **25,** 1137–1140.

——, W. F. Feltz, R. O. Knuteson, H. E. Revercomb, H. B. Howell, and H. M. Woolf, 1999: The retrieval of planetary boundary layer structure using ground-based infrared spectral radiance measurements. *J. Atmos. Oceanic Technol.,* **16,** 323–333.

Speheger, D. A., C. A. Doswell III, and G. J. Stumpf, 2002: The tornadoes of 3 May 1999: Event verification in central Oklahoma and related issues. *Wea. Forecasting,* **17,** 362–381.

Stokes, G., and S. Schwartz, 1994: The Atmospheric Radiation Measurement (ARM) Program: Programmatic background and design of the cloud and radiation test bed. *Bull. Amer. Meteor. Soc.,* **75,** 1201–1221.

Thompson, R. L., and R. Edwards, 2000: Overview of environmental conditions and forecast implications of the 3 May 1999 tornado outbreak. *Wea. Forecasting,* **15,** 682–699.

Tobin, D. C., and Coauthors, 1999: Downwelling spectral radiance observations at the SHEBA ice station: Water vapor continuum measurements from 17 to 26 μm. *J. Geophys. Res.,* **104,** 2081–2092.

Turner, D. D., W. F. Feltz, and R. A. Ferrare, 2000: Continuous water profiles from operational ground-based active and passive remote sensors. *Bull. Amer. Meteor. Soc.,* **81,** 1301–1317.

——, B. M. Lesht, S. A. Clough, J. C. Liljegren, H. E. Revercomb, and D. C. Tobin, 2003: Dry bias and variability in Vaisala RS80-H radiosondes: The ARM experience. *J. Atmos. Oceanic Technol.,* **20,** 117–132.

Wang, J., H. L. Cole, D. J. Carlson, E. R. Miller, K. Beierle, and A. Paukkunen, 2002: Corrections of humidity measurement errors from the Vaisala RS80 radiosonde—Application to TOGA COARE data. *J. Atmos. Oceanic Technol.,* **19,** 981–1002.

Weckwerth, T. M., 2000: The effect of small-scale moisture variability on thunderstorm initiation. *Mon. Wea. Rev.,* **128,** 4017–4030.